PHYSICAL REVIEW B VOLUME 11, NUMBER 12 15 JUNE 1975

# Electronic structure of TiFe

D. A. Papaconstantopoulos*
*Naval Research Laboratory, Washington, D. C. 20375*
(Received 3 June 1974)

Self-consistent energy-band calculations for TiFe were performed by the augmented-plane-wave–$X\alpha$ method. The resulting Fermi surfaces, densities of states, and x-ray spectra are consistent with the de Haas–van Alphen measurements of Kamm, and with x-ray, electronic-specific-heat, and isomer-shift measurements.

## I. INTRODUCTION

In the last few years a number of self-consistent band calculations appeared in the literature. Many of them were dealing with pure elements[1] and several others with compounds.[2] In the area of transition-metal compounds the calculations which have been reported until recently were for materials in which the one component is a transition metal and the other C, N, and O. We now present a self-consistent calculation by the augmented-plane-wave (APW) method on a compound whose components, namely, Ti and Fe, are both transition metals. While this work was in progress, Yamashita and Asano[3] published the results of a similar calculation on TiFe, performed by the Green's-function Korringa-Kohn-Rostoker (KKR) method. We have already reported on non-self-consistent calculations of TiFe,[4] and have given a preliminary account[5] of the present results.

In this work we have calculated the energy bands, Fermi surfaces, densities of states, x-ray spectra, the electron-phonon coupling constant, and the isomer shift. The results are compared with the calculation of Yamashita and Asano, with the Fermi-surface experiments of Kamm,[6] and with electronic-specific-heat,[7] isomer-shift,[8] and x-ray[9] measurements.

The intermetallic compound TiFe is a material of considerable technological interest due to its properties of being brittle and hard. Despite the presence of Fe, it is not ferromagnetic. At 50–50 composition, TiFe has an ordered phase and the CsCl structure.[10]

## II. METHOD OF CALCULATION

The nonrelativistic APW method[11] was employed to find the energy bands and wave functions. The starting potential was found in the usual way by superimposing atomic charge densities.[12] The exchange was determined by the $X\alpha$ method[13] which selects the multipler $\alpha$ in such a way so that the total energy of the atom is at a minimum. The values of $\alpha$ used in this work are those of Schwarz,[14] namely 0.716 and 0.711 for Ti and Fe respectively. Outside the APW spheres $\alpha$ was set equal to $\frac{2}{3}$.[2]

The charge density through the $3p$ subshell was kept frozen and only the charge densities corresponding to the $3d$ and $4s$ subshells of both Ti and Fe were recalculated in each cycle of the self-consistency procedure. The radii of the APW spheres were determined in such a way so that at the point of touching spheres the two potentials were equal. This procedure was followed through each cycle so that the APW sphere radii were redetermined after each iteration. It was assumed that convergence was achieved at the ninth iteration when two successive eigenvalues differed by less than 8 mRy for all states. The oscillations in the eigenvalues were damped by averaging charge densities $\sigma(r)$ using the formula $\sigma(r) = F\sigma^{\text{old}}(r) + (1-F)\sigma^{\text{new}}(r)$, where $F$ was varied between 0.7 and 0.9. Each iteration was performed for 64 $\vec{k}$ points in the simple-cubic Brillouin zone. The final potential was used to calculate energy eigenvalues for 512 $\vec{k}$ points in the zone. These results were interpolated to $48\times10^5$ $\vec{k}$ points to find the densities of states.[15]

## III. ENERGY BANDS

Fig. 1 shows the self-consistent (SC) energy bands of TiFe. The usual notation in the simple-cubic Brillouin zone is used. There are two $d$ bands that arise from the overlapping of the Fe and Ti wave functions. In the language of chemistry the lower $d$ band consists of those wave functions which contribute to the bonding while the higher $d$ band contains the antibonding orbitals.[3]

An analysis of the wave functions for the states $\Gamma_1$, $\Gamma_{12}$ and $\Gamma'_{25}$ is given in Table I, where the results of our SC calculations are compared with our non-self-consistent (NSC) ones. One may conclude that the lower $d$ band is strongly associated with the Fe site, and the higher with the Ti site. We will come back to discuss Table I further in Sec. V.

In our earlier calculations[4] of TiFe we treated the constant potential outside the APW spheres in an approximate way, by taking the average over the region between the APW and the Wigner-Seitz spheres. We have now used the Ewald method[16] to determine the constant potential more accurately, and we have repeated our non-self-consistent calculation for the full Slater exchange and $(4s)^1$ configuration (Fig. 2). Although the resulting densities of states do not differ substantially, we observe several changes in the ordering of levels at $X$, $M$, and $R$.

We can take the differences of $M_3 - \Gamma_{12}$ and $\Gamma'_{25} - \Gamma_{12}$ as a measure of the widths of the lower and higher $d$ bands respectively. In Table II, these widths are given for the various calculations of TiFe, of antiferromagnetic Cr,[17] and Fe.[18] Comparing our NSC calculations to the SC ones, we note a narrowing of about 30% and 22% for the lower and higher $d$ bands respectively. Comparing Fig. 1–2, we observe a major disagreement around $X$. That is, the self-consistent results (see discussion of Fermi surface) show an electron surface around $X$ which is missing from the NSC results. On the other hand, our SC results and the SC results of Yamashita and Asano are in very good agreement despite the 10% difference in the exchange parameter $\alpha$. It appears that compounds are less sensitive to $\alpha$ than the pure elements.[1]

Since the TiFe is isoelectronic with Cr, it is interesting to note that the band structure of antiferromagnetic Cr calculated by Asano and Yamashita[17] is closely similar to the present results, including the energy gap along the [111] direction.

The $d$-band width for bcc Fe may be taken to be the difference $H'_{25} - H_{12}$. Recent calculations of Tawii and Callaway,[18] and several previous calculations, all give a $d$-band width somewhat wider for the elemental Fe than TiFe. This is expected to be the case, since the Fe sites are nearest neighbors in the pure metal but next nearest neighbors in the compound. This narrowing of the $d$ band from the elemental metal to the compound was demonstrated more convincingly by Moruzzi *et al.*[19] in their study of several intermetallic compounds having the CsCl structure. They find that the $d$-band width reduces in the compound by a factor of about 2. Since their comparison is based on calculations of the pure elements having the lattice constant of the compound, while our comparison involves different lattice constants, we offer this as the explanation for our results not to be conclusive on this point.

## IV. FERMI SURFACES

Kamm[6] has found, from his de Haas–van Alphen effect measurements, two principal Fermi surfaces. They can be identified in our calculations as a hole surface around $M$ and an electron surface around $X$, and they are shown in Fig. 3. Kamm has used our results to calculate de Haas–van Alphen frequencies and effective masses for

TABLE I. Angular-momentum character of wave functions at $\Gamma$.

| | | | | Lower $d$ band | | | | | | Higher $d$ band | | | |
|---|---|---|---|---|---|---|---|---|---|---|---|---|---|
| | | $\Gamma_1(s)$ | | | $\Gamma_{12}(d)$ | | | $\Gamma'_{25}(d)$ | | $\Gamma_{12}(d)$ | | $\Gamma'_{25}(d)$ | |
| | NSC ($\alpha = 1$) | NSC ($\alpha = 0.71$) | SC | NSC ($\alpha = 1$) | NSC ($\alpha = 0.71$) | SC | NSC ($\alpha = 1$) | NSC ($\alpha = 0.71$) | SC | NSC ($\alpha = 1$) | SC | NSC ($\alpha = 1$) | SC |
| $E(k)$ (Ry) | 0.192 | 0.173 | 0.164 | 0.433 | 0.404 | 0.411 | 0.607 | 0.576 | 0.613 | 0.824 | 0.769 | 1.000 | 0.905 |
| Ti site (%) | 26.5 | 25.9 | 28.4 | 19.0 | 16.9 | 29.2 | 7.2 | 6.3 | 14.8 | 60.7 | 53.7 | 88.6 | 81.7 |
| Fe site (%) | 33.8 | 34.8 | 32.1 | 63.2 | 65.9 | 51.6 | 90.0 | 90.9 | 81.9 | 30.8 | 40.7 | 8.8 | 16.4 |
| Plane wave (%) | 39.5 | 39.3 | 39.4 | 17.3 | 17.1 | 19.1 | 2.3 | 2.3 | 2.8 | 8.0 | 5.2 | 2.0 | 1.5 |

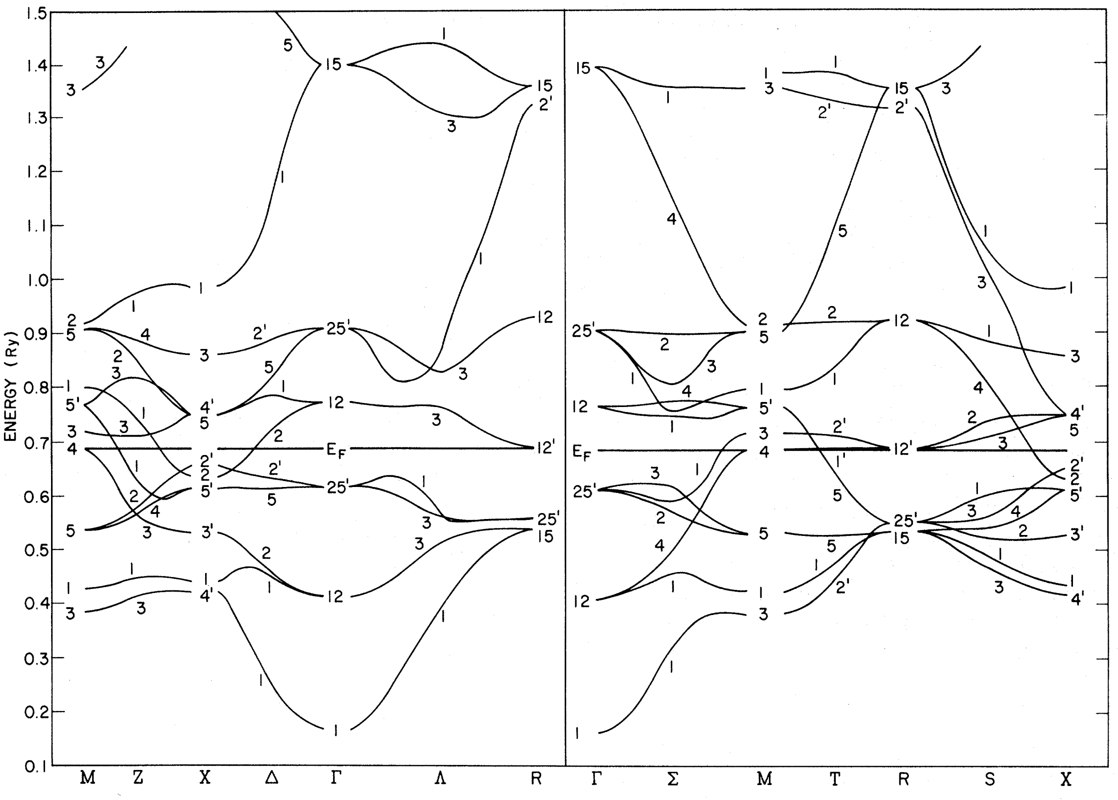

FIG. 1. Self-consistent energy bands of TiFe, with $X\alpha$ exchange.

these surfaces.

A comparison with his measurements is given in Table I of his paper. The volumes enclosed by the calculated Fermi surfaces are about 2.7 times greater than the observed values. Our calculation also produces additional surfaces around $M$ and possibly around $R$, where the energy bands lie very close to the Fermi level. Due to their large effective mass and small size these were not observed by Kamm.

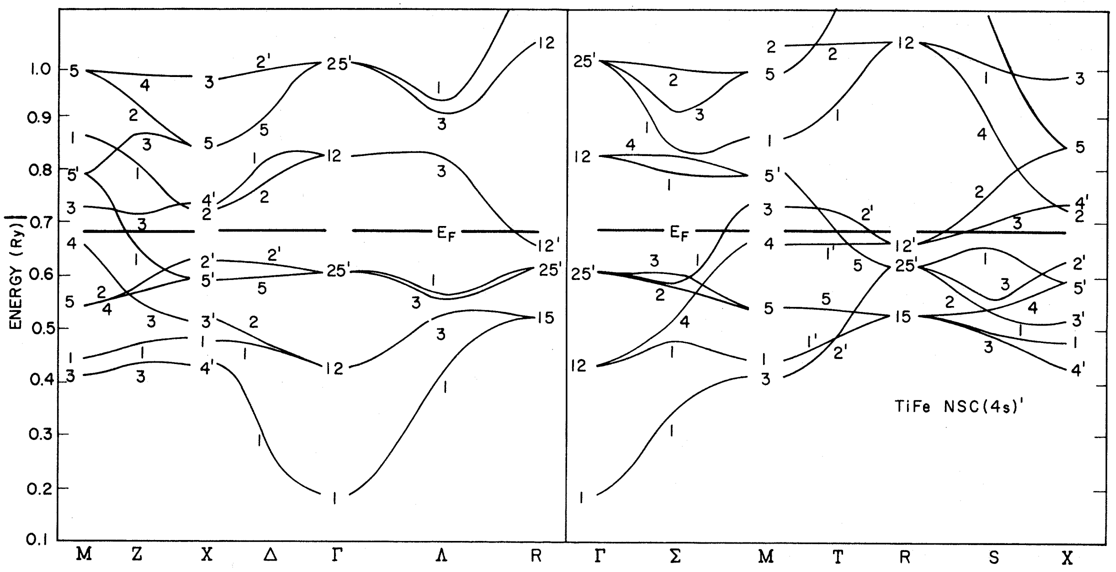

FIG. 2. Non-self-consistent energy bands of TiFe with full Slater exchange.

TABLE II. Comparison of 3*d* band widths.

| | | Lower band (Ry) | Higher band (Ry) |
|---|---|---|---|
| Present results | TiFe NSC $\alpha = 1.0$ | 0.298 | 0.176 |
| | TiFe SC $\alpha = 0.71$ | 0.307 | 0.136 |
| Yamashita and Asano[a] | TiFe SC $\alpha = 0.80$ | 0.292 | 0.129 |
| Asano and Yamashita[b] | Cr SC $\alpha = 0.50$ | 0.251 | 0.102 |
| Tawil and Callaway[c] | Fe SC $\alpha = 0.64$ | 0.37 | ··· |

[a] Reference 3. [b] Reference 17. [c] Reference 18.

We attribute the discrepancy between theory and experiment to the following: (a) the exchange parameters $\alpha$ used in this calculation are the optimum ones for the atoms but not necessarily for the crystal, (b) the "frozen core" approximation may produce some shift of the valence bands, (c) the muffin tin approximation may introduce more shifting, and (d) uncertainties in the interpretation of the de Haas–van Alphen data because of specimen imperfections.

## V. DENSITIES OF STATES AND x-RAY SPECTRA

We have used an interpolation procedure similar to that of Mueller,[15] to obtain the total density of states (DOS) and DOS decomposed per site and per angular momentum component. The decomposed DOS are found from the expression[20]

$$N_\ell^A(E) = \sum_n \int_s \frac{Q^A_{n,\ell}(\vec{k})}{|\nabla E_n(\vec{k})|} , \qquad (1)$$

where $Q^A_{n,\ell}(\vec{k})$ is the electronic charge of atom *A* within the APW sphere.[21] Since $Q^A_{n,\ell}(\vec{k})$ and therefore $N_\ell^A(E)$ are strongly dependent on the crystal wave functions we expect that only self-consistent calculations may produce reliable decomposed DOS. The resulting histograms are presented in Fig. 4. We observe, in agreement with Table I, that below the Fermi level the Fe site has the greater contribution to the total DOS, while above the Fermi level Ti is the main contributor. Table I also indicates the necessity of carrying such calculations to self-consistency, since the electronic

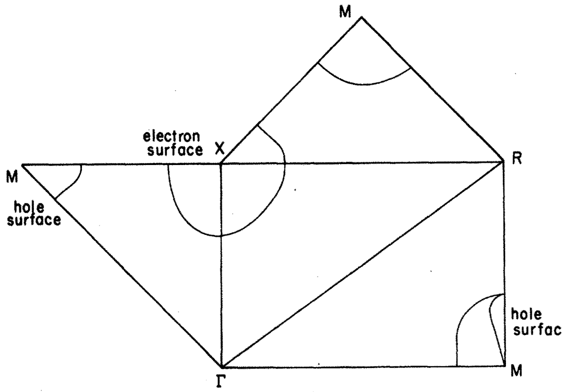

FIG. 3. The intersection of the calculated Fermi surface of TiFe with an elementary tetrahedron having $\frac{1}{48}$ of the volume of the Brillouin zone.

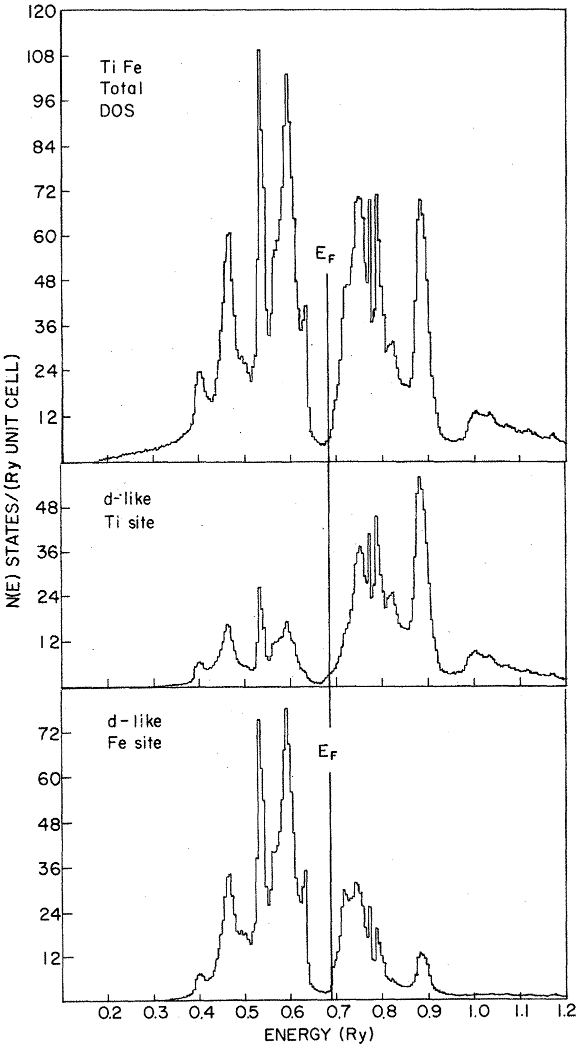

FIG. 4. Total and *d*-like densities of states of TiFe.

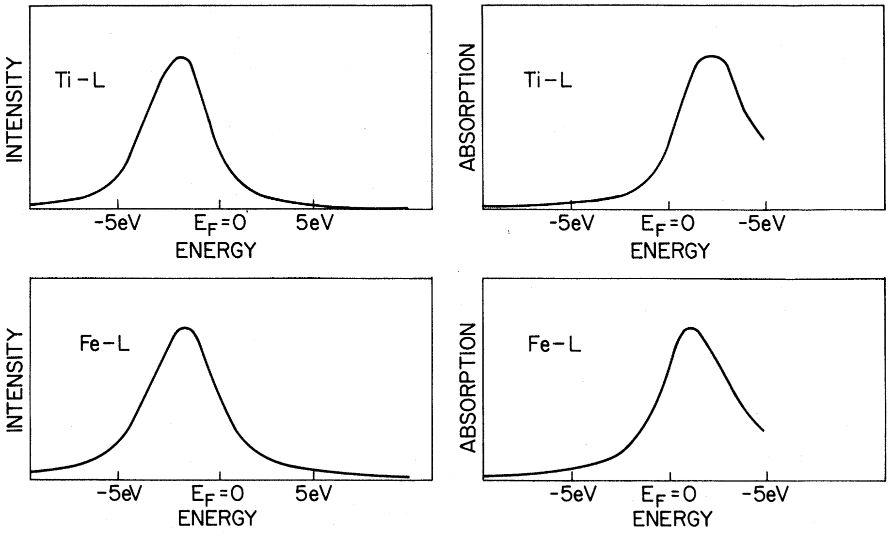

FIG. 5. *L* emission and absorption spectra for both sites of TiFe. All graphs are normalized to the same arbitrary maximum height.

charges differ in some cases between SC and NSC calculations, by as much as a factor of 2.

The x-ray spectrum of a site *A* is proportional to the product

$$N_\ell^A(E)\,|M(n,\ell+1;\ \ell)|^2\,, \tag{2}$$

where $M^2$ is the probability of transition to the core states from the occupied band for emission spectrum and to the unoccupied band for absorption spectrum. We have previously given[5] the *K*-x-ray spectra of TiFe. We have now also calculated the *L*- and *M*-x-ray spectra which involve the $2p$ and $3p$ core states and the *s*- and *d*-like conduction-band states. The results for emission and absorption in both sites of TiFe are shown in Fig. 5–6. They were obtained using Eq. 2 and broadened by an energy-dependent Lorentzian function. This broadening function included a spectrometer distortion function, a core-level broadening, and an electron-lifetime broadening of the form $\frac{1}{4}(E_F-E)^2$, where $E_F$ is the Fermi level and $E$ is the band energy, expressed in rydbergs. The widths of the broadening used were found from Sevier[22] and are given in Table III. Unfortunately, the author is not aware of any measurements of *L* or *M* spectra. Comparison between theory and experiment was made for the *K* spectra in Ref. 5 and yielded very good agreement.[9]

## VI. ELECTRON-PHONON INTERACTION

We have used the theory of Gaspari and Gyorffy[23] to calculate the electron-phonon mass enhance-

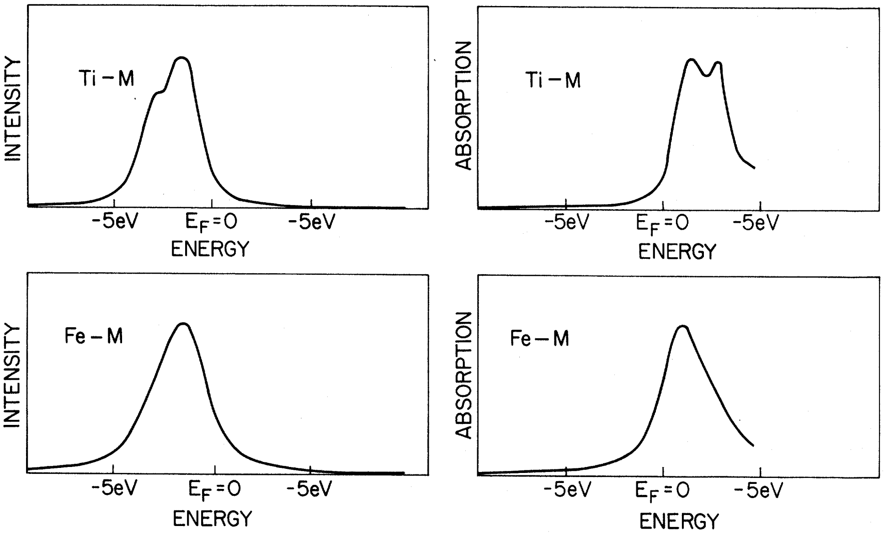

FIG. 6. *M* emission and absorption spectra for both sites of TiFe. All graphs are normalized to the same arbitrary maximum height.

TABLE III. Widths (eV) used in computing x-ray spectra.

| | $K$ spectra (eV) | $L$ spectra (eV) | $M$ spectra (eV) |
|---|---|---|---|
| Spectrometer | 0.4 | 0.6 | 0.1 |
| Core Ti | 1.0 | 0.8 | 0.4 |
| Core Fe | 1.1 | 1.4 | 0.9 |

ment factor $\lambda$. This is given by the following summation, which is a generalization of McMillan's[24] result:

$$\lambda = \sum_A \frac{n(E_F)\langle I^2\rangle_A}{M_A\langle\omega^2\rangle} , \tag{3}$$

where $\langle I^2\rangle_A$ is the square of the electron-phonon matrix element averaged over the Fermi surface, $M$ is the atomic mass and $\langle\omega^2\rangle^{1/2}$ is the average phonon frequency. For $\langle\omega^2\rangle$ we have assumed[24] the value $\Theta_D^2/2$ where $\Theta_D = 495\,^\circ\mathrm{K}$ is the Debye temperature of TiFe,[7] $\langle I^2\rangle_A$ is found from the Gaspari-Gyorffy formula

$$\langle I^2\rangle_A = \frac{E_F}{\pi^2 n(E_F)^2}\sum_\ell \frac{2(\ell+1)\sin^2(\delta_{\ell+1}^A - \delta_\ell^A)\,n_\ell^A n_{\ell+1}^A}{n_\ell^{A(1)}\,n_{\ell+1}^{A(1)}} , \tag{4}$$

where $E_F$ is the Fermi energy with respect to the muffin-tin zero, $\delta_\ell$ is the phase shift, $n_\ell^{A(1)}$ is the free-scatterer density of states, and $n_\ell^A$ is the decomposed DOS defined in Eq. (1). Our results are given in Table IV. The small value of $\lambda = 0.09$ verifies the fact that TiFe is not a superconductor. Indeed applying the McMillan formula[24] we find essentially zero for $T_c$.

We have also used $\lambda$ to obtain the electronic-specific-heat coefficient $\gamma$, from the expression

$$\gamma = (1+\lambda)\tfrac{2}{3}\pi^2 k^2 n(E_F) . \tag{5}$$

The small $\gamma = 0.53$ mJ/mole K$^2$ is consistent with the experiments of Starke *et al.*[7] who reported a small but negative value of $\gamma$ due to the fact that they fitted their specific heat measurements to the following function:

$$C(T) = A + \gamma T + \beta T^3 . \tag{6}$$

## VII. CHARGE TRANSFER AND ISOMER SHIFT

Nevitt[10] suggests that the CsCl-type phases have quasi-ionic bonding, which results from electron transfer associated with the redistribution of electrons in $d$ states. As can be deduced from Table V, our calculation agrees with this explanation. In Table V we compare our charge distribution of the conduction electrons of TiFe with those of Yamashita and Asano. We have decomposed our plane-wave charge outside the APW spheres by assuming it to be proportional to the angular-momentum component of the charge density at the sphere radius.[25] We realize that this decomposition of the outside charges is suspect for Fe where the $d$ state at the Fermi energy is rapidly decaying at the muffin-tin radius. If we substract the total charge assigned to Fe from that of Ti we find 4.36 electrons. This indicates a 0.18 electron transfer from Ti to Fe, $\frac{2}{3}$ of which is $d$-like. In order to compare with the isomer-shift measurements of Mielczarek and Winfree,[8] we have also calculated the electronic charge density at the nucleus for the Fe site of TiFe, to be $\rho_{\mathrm{TiFe}} = 11\,887.093\ a_0^{-3}$. This value is used in the expression

$$\Delta\epsilon = \alpha\,(\rho_{\mathrm{Fe}} - \rho_{\mathrm{TiFe}}) ,$$

where $\Delta\epsilon$ is the isomer-shift difference, $\alpha$ is a constant of proportionality determined by Duff[26] to be

$$\alpha = (-0.23 \pm 0.02)\ a_0^3\ \mathrm{mm\ sec}^{-1}$$

and $\rho_{\mathrm{Fe}} = 11886.154\ a_0^{-3}$ is the electronic charge density at the nucleus for Fe metal as calculated by Wakoh and Yamashita.[27] The result is $\Delta\epsilon = 0.21$ mm/sec. The measured value of Mielczarek and Winfree is $\Delta\epsilon = 0.145$ mm/sec. The discrepancy between theory and experiment may be explained given the fact that our calculation and that of Wakoh and Yamashita differ in the treatment of exchange potential. In addition one should see this result with caution since both of the above calculations did not include relativistic corrections which, in the vicinity of the nucleus, are certainly sizeable even for Fe.

## VIII. COMMENTS ON CERTAIN APPROXIMATIONS USED

To check the criterion of equal potential for the two muffin-tin radii, a calculation was performed

TABLE IV. Densities of states, electron-phonon coupling constant, and coefficient of electronic specific heat.

| | $E_F$ (Ry) | $n_{\text{total}}$ [states/(Ry unit cell spin)] | $n_s$ | $n_p$ | $n_d$ | $n_f$ | $\langle I^2\rangle_A$ [(eV)/Å$^2$] | $\lambda$ | $\gamma$ (mJ/mole K$^2$) |
|---|---|---|---|---|---|---|---|---|---|
| Ti | 0.685 | 2.875 | 0.015 | 0.151 | 1.031 | 0.018 | 2.46 | 0.05 | 0.53 |
| Fe | | | 0.032 | 0.177 | 0.984 | 0.018 | 2.32 | 0.04 | |

TABLE V. Charge distribution of the conduction electrons.

| | | | Inside | | | | | | | | Outside | | | | |
|---|---|---|---|---|---|---|---|---|---|---|---|---|---|---|---|
| | $R$(a.u.) | | $Q_s$ | | $Q_p$ | | $Q_d$ | | $Q_f$ | | $Q_s$ | $Q_p$ | $Q_d$ | $Q_f$ | $Q_{\text{total}}$ |
| | PR[a] | YA[b] | PR | YA | PR | YA | PR | YA | PR | YA | PR | PR | PR | PR | PR |
| Ti | 2.501 | 2.475 | 0.34 | 0.32 | 0.39 | 0.34 | 2.12 | 2.10 | 0.04 | ··· | 0.21 | 0.26 | 0.40 | 0.04 | 3.81 |
| Fe | 2.369 | 2.395 | 0.44 | 0.43 | 0.42 | 0.41 | 6.28 | 6.50 | 0.02 | ··· | 0.24 | 0.31 | 0.45 | 0.02 | 8.17 |

[a] PR: present results.

[b] YA: Yamashita and Asano (Ref. 3).

(for the last potential) with the ionic radii of 2.602 and 2.268 a.u. for Ti and Fe, respectively. The eigenvalues were different by less than 2 mRy. In averaging charge densities using the formula of Sec. II we started with $F = 0.9$ and kept reducing it by 0.05 every other iteration down to $F = 0.7$ for the ninth iteration. After the sixth iteration we did not observe any change in the ordering of states, and the bandwidths did not differ by more than 3 mRy, confirming that adequate convergence was reached.

The only approximation which could modify bands at the Fermi level, is the "frozen core." We have removed this approximation and carried out one extra iteration calculating the $3p$ band of Ti "bandlike" and the rest of the core bands atomiclike. The energy bands near the Fermi level showed a uniform shift of about 10 mRy which did not affect the Fermi surface.

## IX. CONCLUSIONS

In summary, a self-consistent energy-band calculation for the intermetallic alloy TiFe was performed. The results are consistent with the de Haas–van Alphen experiment of Kamm, and with specific-heat and isomer-shift measurements. In addition partial densities of states were produced and x-ray spectra predicted. Finally a comparison was made with the non-self-consistent calculations and the value of performing self-consistent calculations was stressed.

## ACKNOWLEDGMENTS

The author wishes to thank L. S. Birks, B. M. Klein, J. W. McCaffrey, and D. J. Nagel for many useful discussions and suggestions, and E. V. Mielczarek for providing her results prior to publication. He is also indebted to G. N. Kamm for his invaluable assistance in the interpretation of the Fermi-surface results.

---

*Permanent address: George Mason University, Fairfax, Va. 22030.

[1] J. W. D. Connolly, Phys. Rev. 159, 415 (1967); D. A. Papaconstantopoulos, J. R. Anderson, and J. W. McCaffrey, Phys. Rev. B 5, 1214 (1972).

[2] P. Weinberger, K. Schwarz, and A. Neckel, J. Phys. Chem. Solids 32, 2063 (1971); K. Schwarz, Monatsh. Chem. 102, 1400 (1971).

[3] J. Yamashita and S. Asano, Prog. Theor. Phys. 48, 2119 (1972).

[4] D. A. Papaconstantopoulos and D. J. Nagel, Int. J. Quantum Chem. S5, 515 (1972).

[5] D. A. Papaconstantopoulos, Phys. Rev. Lett. 31, 1050 (1973).

[6] G. N. Kamm (unpublished).

[7] E. A. Starke, C. H. Cheng and P. A. Beck, Phys. Rev. 126, 1746 (1962).

[8] E. V. Mielczarek and W. Winfree, Bull. Am. Phys. Soc. 19, 203 (1974); Phys. Rev. B 11, 1026 (1975).

[9] S. A. Nemnonov and K. M. Kolobova, Fiz. Me. Metalloved. 23, 456 (1967) [Phys. Me. Metallogr. 23, No. 3, 66 (1967)]; E. Kalne, J. Phys. F 4, 167 (1974).

[10] M. V. Nevitt, in *Electronic Structure and Alloy Chemistry of the Transition Elements*, edited by P. A. Beck (Wiley, New York, 1963), p. 101.

[11] J. C. Slater, Phys. Rev. 51, 846 (1937).

[12] P. O. Löwdin, Adv. Phys. 5, 1 (1956); L. F. Mattheiss, Phys. Rev. 133, A1399 (1964).

[13] J. C. Slater and J. H. Wood, Int. J. Quantum Chem. 4S, 3 (1971); J. C. Slater, *ibid.* 5S, 403 (1972).

[14] K. Schwarz, Phys. Rev. B 5, 2466 (1972).

[15] F. M. Mueller, J. W. Garland, M. H. Cohen, and K. H. Bennemann, Ann. Phys. (N. Y.), 67, 19 (1971).

[16] P. P. Ewald, Ann. Phys. (Leipz.) 64, 253 (1921); J. C. Slater, *Quantum Theory of Molecules and Solids* (McGraw-Hill, N. Y. 1967), Vol. 3, Chap. 9.

[17] S. Asano and J. Yamashita, J. Phys. Soc. Jpn. 23, 714 (1967).

[18] R. A. Tawil and J. Callaway, Phys. Rev. B 7, 4242 (1973).

[19] V. L. Moruzzi, A. R. Williams, and J. F. Janak, Phys. Rev. 10, 4956 (1974).

[20] J. W. McCaffrey and D. A. Papaconstantopoulos, Solid State Commun., 14, 1055 (1974).

[21] L. F. Mattheiss, J. H. Wood, and A. C. Switendick, Methods Comput. Phys. 8, 63 (1968).

[22] K. D. Sevier, *Low Energy Electron Spectrometry* (Wiley, New York, 1972).

[23] G. D. Gaspari and B. L. Gyorffy, Phys. Rev. Lett. 28, 801 (1972).

[24] W. L. McMillan, Phys. Rev. 167, 331 (1968).

[25] E. A. Kmetko, Natl. Bur. Std. (U.S.) Spec. Publ. No. 323 (U. S. GPO, Washington, D.C., 1971), p. 67.

[26] K. J. Duff, Phys. Rev. B 9, 66 (1974).

[27] S. Wakoh and J. Yamashita, J. Phys. Soc. Jpn. 25, 1272 (1968).